

See discussions, stats, and author profiles for this publication at: <https://www.researchgate.net/publication/256450832>

# In Situ Analysis of Heterogeneity in the Lipid Content of Single Green Microalgae in Alginate Hydrogel Microcapsules

ARTICLE *in* ANALYTICAL CHEMISTRY · SEPTEMBER 2013

Impact Factor: 5.64 · DOI: 10.1021/ac401836j · Source: PubMed

---

CITATIONS

11

---

READS

18

4 AUTHORS, INCLUDING:



Do-Hyun Lee

University of California, Irvine

9 PUBLICATIONS 93 CITATIONS

SEE PROFILE

# In Situ Analysis of Heterogeneity in the Lipid Content of Single Green Microalgae in Alginate Hydrogel Microcapsules

Do-Hyun Lee,<sup>†</sup> Chae Yun Bae,<sup>†</sup> Jong-In Han,<sup>‡</sup> and Je-Kyun Park<sup>\*,†,§</sup>

<sup>†</sup>Department of Bio and Brain Engineering, Korea Advanced Institute of Science and Technology, 291 Daehak-ro, Yuseong-gu, Daejeon 305-701, Republic of Korea

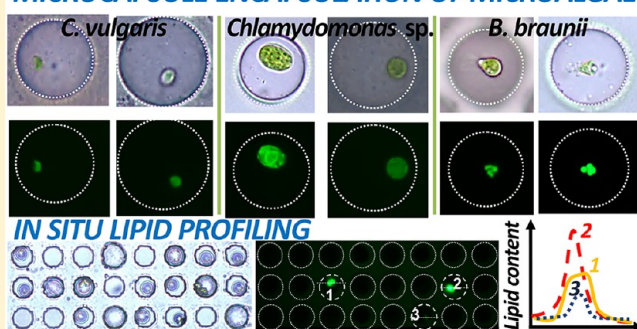
<sup>‡</sup>Department of Civil and Environmental Engineering, Korea Advanced Institute of Science and Technology, 291 Daehak-ro, Yuseong-gu, Daejeon 305-701, Republic of Korea

<sup>§</sup>KAIST Institute for the NanoCentury, 291 Daehak-ro, Yuseong-gu, Daejeon 305-701, Republic of Korea

## S Supporting Information

**ABSTRACT:** Microalgae, a group of microorganisms that grow using sunlight as the sole energy source and carbon dioxide as an only carbon source, have been considered as a feedstock of choice for the production of biofuels such as biodiesel. To explore the economic feasibility of such application, however, many technical hurdles must first be overcome; the selection and/or screening of competent species are some of the most important and yet challenging tasks. To greatly accelerate this rather slow and laborious step, we developed a droplet-based microfluidic system that uses alginate hydrogel microcapsules with a mean diameter of 26  $\mu\text{m}$ , each of which is able to encapsulate a single microalgal cell. This novel device was successfully demonstrated using three microalgae species, namely, *Chlorella vulgaris*, *Chlamydomonas* sp., and *Botryococcus braunii*. In situ analysis of the lipid content of individual microalgal cells by nondestructive fluorescence staining using BODIPY (4,4-difluoro-1,3,5,7-tetramethyl-4-bora-3a,4a-diaza-s-indacene) was possible. In all cases, we confirmed that the lipid content of microalgal species in alginate hydrogel microcapsules was comparable to that of free-living cells. Stochastic heterogeneity in the lipid content was verified under a highly viable physiological condition, implying that other analyses were possible after the determination of lipid content. Furthermore, the designed microwell arrays enabled us to distinguish the BODIPY fluorescence response of a single live alga within the microcapsules.

### MICROCAPSULE ENCAPSULATION OF MICROALGAE



In response to the skyrocketing prices of fossil fuels and the sudden acceleration of global warming by the greenhouse effect over the past few decades, substantial concerns have prompted the discovery and development of alternative energy sources.<sup>1</sup> Biofuels, such as biodiesel from microalgae, have drawn increasing attention as a potential alternative to fossil energy due to their sustainable nature.<sup>2</sup> However, many issues remain to be solved, mainly regarding the economic viability of biofuels, before realizing commercial production<sup>3</sup> and the recovery of microalgal biomass.<sup>4</sup> The isolation of high-performance strains, e.g., lipid-rich and yet fast-growing cells (or cells with superb lipid productivity), is one such issue.<sup>5,6</sup> To this end, it is a current practice that the lipid productivity of species is compared in a batch and lump sum manner. In this way, however, any differences at the single-cell level even among the same species and batch, which in fact exist, cannot be considered. The ability to identify and isolate a single cell, particularly in a rapid and high-throughput manner, becomes even more important in screening mutants with high lipid productivity.<sup>7</sup>

Microfluidics has driven innovations in biological research, exploiting several advantages of the unique fluidic behavior through sophisticated control within precisely fabricated microstructures. Even at the single-cell level, multiplexed biological experiments have been demonstrated using high-throughput microfluidic analysis.<sup>8,9</sup> Recently, some interesting microalgae research has been reported, including their use as miniaturized sensing devices for environmental pollution,<sup>10,11</sup> photobioreactors for biofuel production,<sup>12</sup> and cell culture devices for microalgae screening.<sup>13,14</sup> In fact, microfluidic devices make it possible to accomplish numerous algae-based studies that are challenging or even impossible to achieve using their macrosized counterparts. One such task is the selection and/or screening of potent microalgae, e.g., cells with high lipid productivity, which is presented here.

Sophisticated tools for single-cell analysis based on a wide range of new microtechnologies have emerged in the past

Received: June 18, 2013

Accepted: August 16, 2013

Published: August 16, 2013

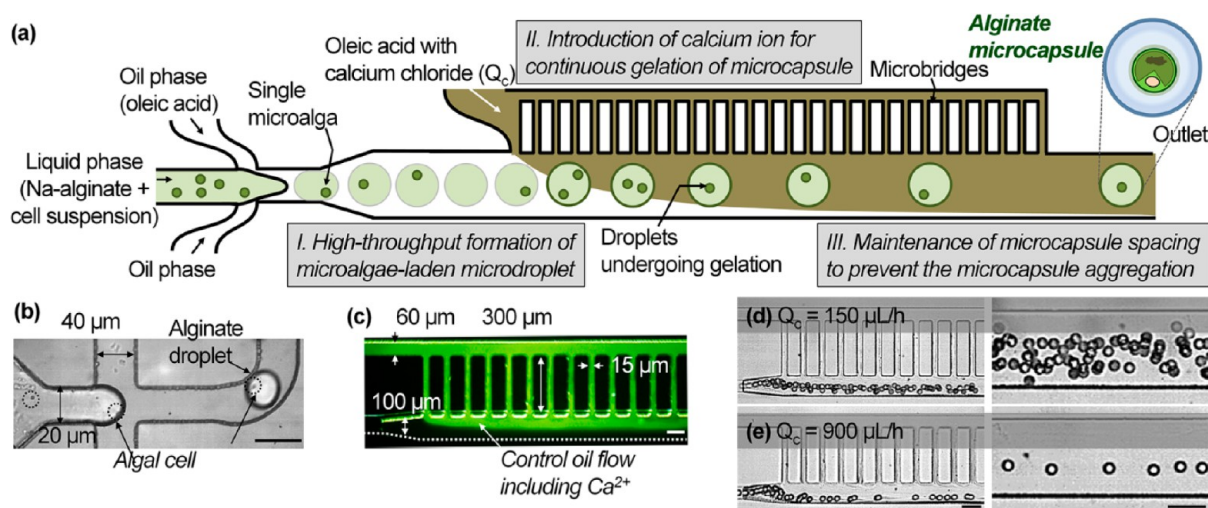


**Figure 1.** Design and operating principles for the rapid preparation of monodispersed alginate hydrogel microcapsules encapsulating algal cells. (a) Schematic diagram of the microfluidic device with integrated microbridge structures for the generation of alginate hydrogel microcapsules containing algal cells with sufficient spacing. (b) Bright-field micrograph showing cell encapsulation into a sodium alginate droplet at the cross junction. (c) Fluorescence micrograph illustrating the migration of control flow passing through each microbridge. The additional control oil flow ( $Q_c$ ), including calcified oleic acid, changes the velocity of the main flow via the microbridge structures. (d and e) Micrographs showing variation in droplet interval within the main channel (left panels) and near the outlet (right panels) at  $Q_c$  of (d) 150 or (e) 900  $\mu\text{L}/\text{h}$ . Scale bars: 50  $\mu\text{m}$ .

decade.<sup>15</sup> Optical<sup>16</sup> and magnetic tweezers<sup>17</sup> have unique strengths of high resolution and the capability of three-dimensional manipulation, but they require complex optical systems and high optical energy. Microwell arrays, miniaturized replicas of 96-well plates, allow cells to be localized and monitored at the single-cell level.<sup>18</sup> This approach, however, has not been applied to microalgae, primarily due to the small cell size. A feasible alternative would be microdroplet-based technologies, which exploit droplets as tiny-volume units of fluid that are enveloped by immiscible fluid, such as oil, and have resulted in a state-of-the-art method of isolation and encapsulation of individual cells for a variety of purposes.<sup>19–22</sup> Highly monodispersed droplets of micro-sized diameter can be produced rapidly;<sup>23</sup> thus, a single cell can be encapsulated within a well-controlled microenvironment inside the droplet.

The applicability of droplet-based microfluidics can be improved substantially by the synthesis and assembly of hydrogel microcapsules.<sup>24</sup> Hydrogels are an exciting class of scaffolding polymer that have great potential in biomedical applications due to their high biocompatibility, smart-response nature to the local environment, and ease of cross-linking under mild reaction conditions. Hydrogel microcapsules, when loaded with cells, are transported to the target site in an effective way and allow manipulation of cells with high viability and cultivability.<sup>25</sup> Alginate is an excellent material that is preferred over other hydrogel precursors for the entrapment of a single microalga due to its biodegradability, rapid solidification using calcium ions, and high permeability to nutrients. Several groups have exploited microfluidics for the encapsulation of cells in spherical alginate microcapsules. Morimoto et al. reported an internal gelation process with  $\text{CaCO}_3$  nanoparticles;<sup>26</sup> however, there was a drawback in terms of reduced viability due to gradual diffusion of acetic acid. Also, despite their monodispersity and spherical shape, the fabricated microcapsules were relatively large ( $\sim 100\ \mu\text{m}$ ), making them inappropriate for encapsulation of a single small microalga. To date, the bulk immobilization of green microalgae has been demonstrated for only in situ monitoring of metal ion adsorption<sup>27</sup> and the

assessment of eutrophication in flowing waters.<sup>28</sup> An attempt was made to encapsulate a type of algae into hydrogel microcapsules to enable continuous tracking of their motility,<sup>26</sup> although no cell screening on the basis of lipid productivity has yet been reported.

Herein, we demonstrate the encapsulation of high-level biodiesel-producing microalgae into an alginate hydrogel microcapsule based on droplet-based microfluidics, as well as the in situ analysis of lipid content at the single-cell level. The picoliter-sized alginate hydrogel microcapsules, which were generated with high throughput and high uniformity, serve as a smart identification card that contains a biometric signature, which comprises parameters including phenotype, lipid content, and viability. The proposed technique provides the following advantages over conventional liquid droplets: (i) microcapsules containing single cells can be manipulated for long periods of time with little evaporation of medium, (ii) the microcapsules can be utilized with microcapsule-based assay systems for further cell research, and (iii) the trapped individual cell, when necessary, can be recovered easily from the alginate microcapsule by dissolving it in biocompatible buffer. To detect intercellular lipids and compare them among microalgal strains, we utilized a lipophilic bright green fluorescent dye, BODIPY 505/515. BODIPY staining is a nondestructive means of lipid determination in live algal cells. Because the stained cells are viable, further analyses are also possible.<sup>29</sup> In this study, we encapsulated single cells of three green microalgae species (*Chlorella vulgaris*, *Chlamydomonas* sp., and *Botryococcus braunii*) in monodispersed microcapsules and conducted an in situ comparison and analysis of heterogeneity in the lipid contents of individual cells within the microcapsules by staining with BODIPY dye. In addition, we designed the high-density microwell arrays for inserting cell-encapsulating microcapsules and successfully observed the BODIPY fluorescence responses of the different single live algae.



## ■ EXPERIMENTAL SECTION

**Design and Fabrication of Microchannels.** A microcapsule generator with integrated microbridge structures (Figure 1a) was fabricated in poly(dimethylsiloxane) (PDMS) by soft lithography. This device consisted of two channels for sodium alginate and oil (20 and 40  $\mu\text{m}$  wide, respectively), the microbridge (15  $\mu\text{m}$  wide and 300  $\mu\text{m}$  long), the main channel (100  $\mu\text{m}$  wide), and a diverging microchannel near the outlet (200  $\mu\text{m}$  wide). A PDMS mold was obtained by patterning SU-8 photoresist (Microchem Corp., St. Newton, MA) on a silicon wafer using standard lithography. Liquid PDMS mixed with a curing agent (ratio of 7:1) was cast on the mold and cured for 3 h in a convection oven at 65  $^{\circ}\text{C}$  for complete cross-linking. The PDMS microchannel was irreversibly sealed with a glass slide after exposure to oxygen plasma for 30 s. As the hydrophobic PDMS surface of the microchannel became hydrophilic during plasma treatment, the microfluidic device was stored in a convection oven at 65  $^{\circ}\text{C}$  for 1 day to allow recovery of the hydrophobic nature of the microchannel. After the fabrication process, the microfluidic devices were sterilized with 1% (w/v) Pluronic F127 in distilled water prior to cell loading without algal cell attachment. Subsequently, the microchannels were flushed with an oil phase. A microwell array was fabricated with a ultraviolet (UV)-curable negative photoresist, THB-126N (JSR Corp., Japan), on the glass slide. THB-126N photoresist was spin-coated on the glass substrate and prebaked. THB-126N photomask was exposed to UV light through the film-based photomask patterned for the microwell array, followed by developing and rinsing. A 120  $\mu\text{m}$  thick adhesive tape was used as a spacer. After the removal of excess microcapsules, the microwells were sealed with a cover glass to confine the microcapsules.

**BODIPY-Stained Algal Cell Preparation.** *C. vulgaris* was cultivated at 20  $^{\circ}\text{C}$  in nonsaline BG 11 medium. *Chlamydomonas* sp. (KMMCC-1681) and *B. braunii* (KMMCC-868) were obtained from the algal culture collection at the Korean Marine Microalgae Culture Center (Busan, Korea). *Chlamydomonas* sp. and *B. braunii* were grown in JM medium prepared in sterilized natural freshwater. All cultures were incubated under constant shaking with an agitation speed of 120 rpm and continuous illumination with a 3000-lx intensity lamp. BODIPY 505/515 (4,4-difluoro-1,3,5,7-tetramethyl-4-bora-3a,4a-diaza-s-indacene; Invitrogen Molecular Probes, Carlsbad, CA) was dissolved in dimethyl sulfoxide (DMSO) to prepare a stock solution of 100 mg/L. Incubation for 30 min in darkness at room temperature was used for all staining. BODIPY 505/515-stained cells were examined microscopically using an inverted epifluorescence microscope (IX51; Olympus, Tokyo, Japan).

**Preparation of Monodisperse Alginate Hydrogel Microcapsules Encapsulating Algal Cells.** Sodium alginate (1% w/w; A0682-100G, Sigma) in JM media was prepared and filtered with a 0.22  $\mu\text{m}$  syringe filter (Millex-GV, Millipore) to remove any clumps of alginate. Oleic acid (Sigma) with Abil EM 90 surfactant (4% w/w) was introduced as a continuous phase, and the sodium alginate was cross-linked by the calcified oleic acid (24 mg/mL). The calcified oleic acid was prepared by dissolving 0.6 g of calcium chloride (C7902-500G, Sigma) in 25 mL of oleic acid via ultrasonication. Calcium chloride was dissolved in 25 mL of 2-methyl-1-propanol (J.T. Baker, Deventer, The Netherlands) via ultrasonication. After mixing calcium chloride and oleic acid at a ratio of 50% (v/v), the 2-methyl-1-propanol was distilled in a convection oven at 65  $^{\circ}\text{C}$

for a day. All fluids were injected and transported via syringe pumps (Pump 11 Pico Plus; Harvard Apparatus, Inc., Holliston, MA) at a range of volumetric flow rates.

**Cell Viability Assay.** As a general staining method to determine cell viability, dual-fluorescence viability assays using nucleic-acid-binding fluorescent probes, such as SYTO and propidium iodide, have been used widely. Due to the autofluorescence of chlorophyll pigments, however, these assays could not be used in this study. Therefore, SYTOX green, which is used predominantly for staining phytoplankton species and can penetrate damaged cell membranes, was used. Because SYTOX green fluorescence does not overlap with the red autofluorescence, the dead microalgae—which exhibit bright green fluorescence—could be distinguished easily. Cell viability was measured at 3 h after the encapsulation of cells.

## ■ RESULTS

**High-Throughput Production of Alginate Hydrogel Microcapsules Encapsulating Microalgal Cells.** To fabricate the algae cell capsules, we used a previously developed microfluidic device with integrated microbridge structures (Figure 1a).<sup>30</sup> Briefly, the microbridge provides two advantages in microcapsule preparation: (i) the aggregation of surrounding microcapsules can be prevented by suitable microfluidic spacing, and (ii) the size of droplets can be maintained irrespective of the control flow rate ( $Q_c$ ). We dispersed microdroplets of sodium alginate in media containing an alga in a continuous phase of oleic acid with Abil EM 90 surfactant (4% w/w) using a flow-focusing method at a cross junction (Figure 1b). To generate spherical hydrogel microcapsules, we exploited the enlargement in channel height from 35 to 100  $\mu\text{m}$ , which facilitated recovery of the droplet shape from a plug to a sphere. Further downstream, the additional control oil flow ( $Q_c$ ), which includes calcified oleic acid (24 mg/mL) with a surfactant, changes the velocity of the main flow via the microbridge structures. We could visualize the migration of control flow by means of the autofluorescence of calcified oil passing through each microbridge (Figure 1c). The control flow occupied more space in the microchannel when  $Q_c$  increased (Figure 1, parts d and e), showing good agreement with the simulation, as reported previously.<sup>30</sup> As a result, the droplet interval can be adjusted actively within the main channel and near the outlet, when  $Q_c$  is 150  $\mu\text{L}/\text{h}$  (Figure 1d) or 900  $\mu\text{L}/\text{h}$  (Figure 1e).

Parts a and b of Figure 2 present enlarged images of the fabricated cell-laden spherical microcapsule with different spacing under  $Q_c$  values of 150 and 900  $\mu\text{L}/\text{h}$ , respectively. Undesirable coalescence of the hydrogel microcapsule was observed at the relatively low control flow rate. As a result, we confirmed that suitable spacing between two approaching microdroplets guaranteed the stable formation of alginate hydrogel microcapsules. This unwanted coalescence and aggregation of hydrogel microcapsules due to insufficient spacing reduces both monodispersity and single-cell encapsulation efficiency, despite the presence of a surfactant layer. Through temporal control by adjusting the spacing between two microcapsules, we successfully fabricated spherical alginate microcapsules containing a single algal cell with no aggregation.

Figure 2c shows that the droplet interval increased significantly as  $Q_c$  increased without any effect on the droplet-generating pattern. When  $Q_c$  was adjusted from 150 to 900  $\mu\text{L}/\text{h}$ , the droplet interval changed from  $34.40 \pm 12.14$

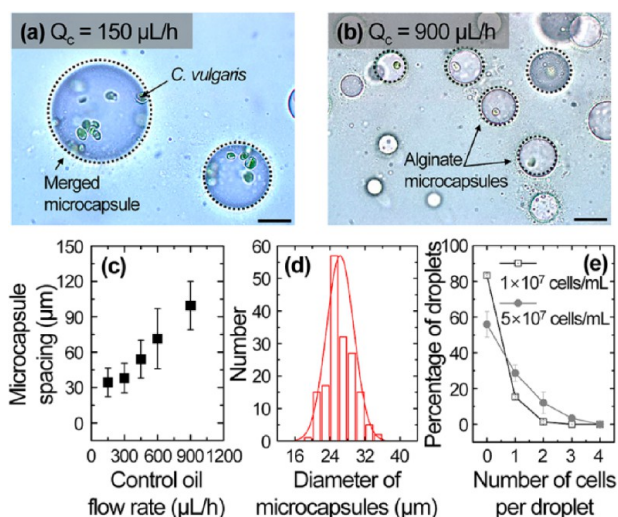


**Figure 2.** (a and b) Enlarged images of a fabricated cell-laden spherical microcapsule with different spacing under control flow rates ( $Q_c$ ) of (a) 150 and (b) 900  $\mu\text{L/h}$ . Aggregation of hydrogel microcapsules occurred at relatively low  $Q_c$ . Scale bars: 25  $\mu\text{m}$ . (c) Microdroplet interval near the outlet according to  $Q_c$ . (d) Diameter distribution of alginate droplets shown under flow conditions of  $Q_w = 20 \mu\text{L/h}$  and  $Q_o = 50 \mu\text{L/h}$ . The generated alginate droplets were monodispersed with a mean diameter of 26.34  $\mu\text{m}$ . (e) Percentage of droplets containing single *C. vulgaris* cells at initial cell loading concentrations of  $1 \times 10^7$  and  $5 \times 10^7$  cells/mL. Up to 35% of droplets contained single algal cells.

to  $99.52 \pm 20.48 \mu\text{m}$ , at a fixed droplet generation condition with a sodium alginate flow rate ( $Q_w$ ) of 20  $\mu\text{L/h}$  and oil flow rate ( $Q_o$ ) of 50  $\mu\text{L/h}$ .

We produced monodispersed sodium alginate droplets within the microchannel. Figure 2d illustrates the variability in droplet size with a flow rate ratio ( $Q_w/Q_o$ ) of 0.4 when generating alginate droplets containing *C. vulgaris*. We utilized oleic acid with the Abil EM 90 surfactant (4% w/w) as the oil phase and cell medium (BG 11 for *C. vulgaris* and JM for *Chlamydomonas* sp. and *B. braunii*) containing sodium alginate (1% w/w) as the liquid phase. The microcapsules showed high monodispersity irrespective of the presence of a cell. The oil flow rate was fixed at 50  $\mu\text{L/h}$ . We could adjust the microcapsule diameter from 19 to 36  $\mu\text{m}$ . As the flow rate ratio increased, the droplet diameter decreased (data not shown). As depicted in Figure 2d, we generated monodispersed algal-cell-encapsulating alginate droplets with a mean diameter of 26.34  $\mu\text{m}$  ( $n = 170$ ). We confirmed that the percentage of single-cell-containing droplets at initial cell loading concentrations of  $1 \times 10^7$  and  $5 \times 10^7$  cells/mL was similar to the theoretical value of the Poisson distribution. Using the proposed device, up to 35% of droplets generated contained single algal cells (Figure 2e). The efficiency of single-cell encapsulation could be enhanced by incorporating the interconnection technique or secondary microfluidic networks.<sup>31</sup>

**Microcapsule-Based Interspecies Comparison of the Intracellular Lipids in Microalgae.** Lipid productivity, which is calculated based on both the growth and lipid content of oleaginous microbes such as microalgae, is advantageous for microalgae-derived biodiesel production.<sup>6</sup> Obtaining microalgal species with such properties is critical; however, doing so is challenging, particularly in a high-throughput manner. To

investigate the lipid content of a cell encapsulated within an alginate hydrogel microcapsule, the BODIPY fluorescent dye was employed and three microalgal species were investigated (Figure 3). Nile red, which stains lipids within animal cells and

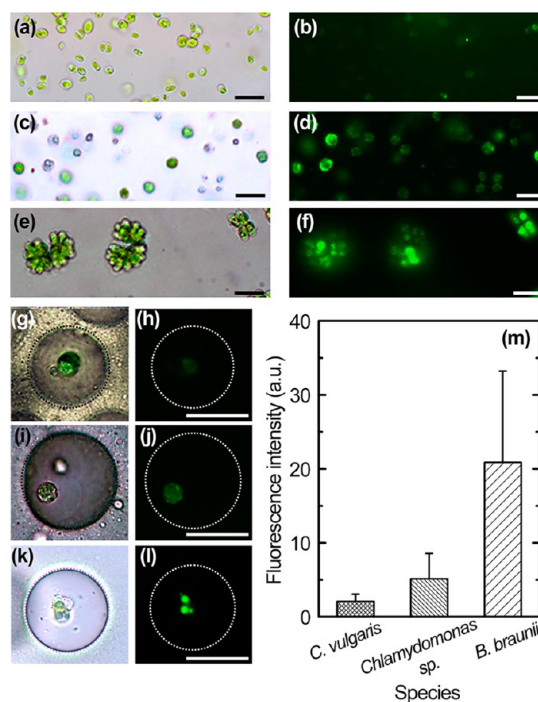


**Figure 3.** Bright-field and fluorescence images of (a and b) *C. vulgaris*, (c and d) *Chlamydomonas* sp., and (e and f) *B. braunii* cells, respectively, stained with BODIPY in bulk. Enlarged bright-field and fluorescence images of freely suspended microcapsules containing single (g and h) *C. vulgaris*, (i and j) *Chlamydomonas* sp., and (k and l) *B. braunii* cells, respectively. Scale bars: 20  $\mu\text{m}$ . (m) The average fluorescence intensity profiles of each species of the three microalgae within microcapsules ( $n = 60$ ).

microorganisms, was not suitable for this study, as it is unable to penetrate the thick walls of microalgal cells and both the dye itself and/or a carrier solvent are detrimental to cell viability; further, its emission spectrum overlaps with that of chlorophyll, so it interferes with accurate estimation of intercellular lipids. After staining with BODIPY, the lipid bodies in all three algal cells exhibited bright green fluorescence, although the intensity varied markedly (Figure 3, parts b, d, and f).

Bright-field microscopic images of freely suspended microcapsules containing single cells of three species were obtained in the microfluidic device (Figure 3, parts g, i, and k). It was hard to get an accurate measurement of lipid production within multicell-containing (>2 cells) microcapsules because there might be an overlap among the fluorescence signal of each microalga. Even if it seems a bit confusing by the existence of a satellite cell in Figure 3i, all results of in situ measurement of the lipid content were gathered from the single-cell-containing microcapsules, except for multicell-containing microcapsules which account for ~15% of the generated microcapsules. The positions of cells inside the microcapsules varied due to the circulation flow within the droplet before gelation. To confirm and compare lipid accumulation of a single cell of among three species, we visualized the green fluorescence within the microcapsules by fluorescence microscopy (Figure 3, parts h, j, and l). The lipid measurement was performed immediately



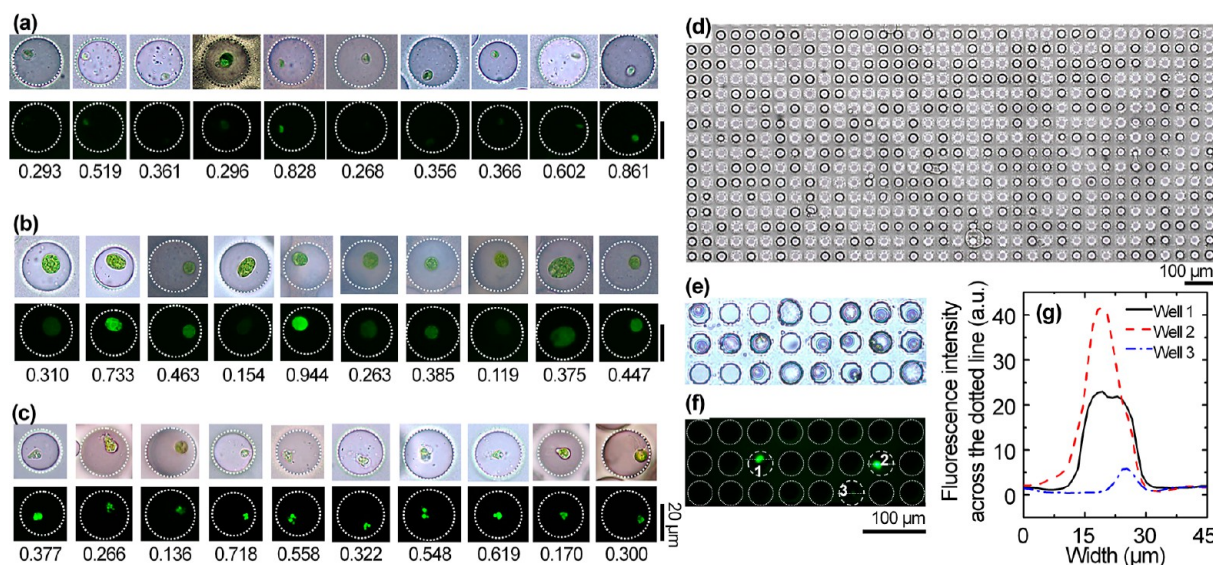


**Figure 4.** Microcapsule-based in situ profiling of the lipid contents of three microalgae species within hydrogel microcapsules at the single-cell level. Enlarged bright-field and fluorescence images of microcapsules containing single cells stained with BODIPY: (a) *C. vulgaris*, (b) *Chlamydomonas* sp., and (c) *B. braunii*, respectively. The normalized fluorescence intensities noted at bottom indicate the heterogeneity in lipid content. (d) Micrograph of the hydrogel microcapsule array. Hydrogel microcapsules containing single *B. braunii* cells were distributed randomly within the high-density microwell array. Magnified (e) bright-field and (f) fluorescence images of a trapped microcapsule. Microcapsules containing single *B. braunii* cells were readily distinguishable from empty microcapsules by fluorescence microscopy. (g) Three different fluorescence responses of single *B. braunii* cells across the dotted line from the trapped microcapsules in each of the microwells shown in panel f.

after the collection of encapsulated microcapsules. The results suggest that the intracellular lipid levels were distinguishable, although the cell was encapsulated in the microcapsule. Figure 3m shows the average fluorescence intensities of the three microalgal species within microcapsules, which is indicative of their average lipid contents. *B. braunii* exhibited higher lipid content than *C. vulgaris* or *Chlamydomonas* sp.

**In Situ Profiling of Heterogeneity in the Lipid Accumulation among Individual Cells.** The conventional method of estimating the lipid content of microalgae represents only the average value of a population. Therefore, any heterogeneity in lipid accumulation is not reflected. Traditionally, the lipid content of microalgae is estimated by measuring the dry biomass via a gravimetric method, which requires at least 10–15 mg wet weight of cells and a day-long drying process. Furthermore, because postextraction algae cannot be subjected to any additional analyses, fluorescence measurement using Nile red<sup>32</sup> and BODIPY<sup>33</sup> staining is more appropriate for single-cell lipid screening. A comparison between the lipid contents measured by Nile red or BODIPY and the lipid content showed a linear relationship, which has advantages of in situ measurement of single microalga within a microcapsule in a high-throughput manner.

To identify heterogeneity among individual cells in a population, we isolated single-cell-containing hydrogel microcapsules and examined their lipid contents by BODIPY staining. The lipid contents of 10 randomly selected single *C. vulgaris*, *Chlamydomonas* sp., and *B. braunii* cells are shown in Figure 4a–c. We successfully generated monodispersed hydrogel microcapsules with a mean diameter of 26 µm, each of which contained a single microalgal cell. Accumulated lipid bodies, which are evident in these images, exhibited highly variable fluorescence signals among cells within each microcapsule. The normalized fluorescence intensity of individual cells within microcapsules is indicated at the bottom of Figure 4a–c. The fluorescence intensity was normalized to the

maximum intensity of each species. Supporting Information Figure S1 shows the results of profiling of whole microcapsules and the fluorescence intensity distribution of individual cells of the three algal species tested. Each fluorescence intensity frequency corresponds to the green fluorescence of individual cells within a single microcapsule. On the basis of these findings, we propose classification of individual algal cells according to their lipid content; e.g., lipid contents on a scale of 0 to 1. Particularly, due to its exceptionally high lipid content, the botryoid-shaped microalgal species *B. braunii* has been considered the feedstock of choice for biodiesel production. Further, *B. braunii* can form blooms; these individual pyriform-shaped cells stand together and contain long hydrocarbon chains. To visualize the lipid contents of individual cells, we disintegrated the clump (or colony) by mild sonication. This physical disruption resulted in BODIPY being localized in lipid globules, which appeared to be round, without other cytoplasmic compartments (Figure 4c). Thus, lipid bodies could be distinguished from other parts of the cell as bright green structures, even though the individual microalga was encapsulated in the hydrogel microcapsule. The greater green fluorescence intensity, which indicates higher lipid content, indicates that *B. braunii* is a potent lipid producer.

We constructed a microwell array with single microalga-containing microcapsules (Figure 4d). Each microwell had a width, depth, and center-to-center distance of 35, 17, and 50 µm, respectively. In total, ~110 000 wells were present on a 15 × 15 mm<sup>2</sup> substrate. Microcapsules filled ~60% of the microwell array. Use of a microstructure for more efficient insertion of microcapsules into microwells could allow ~95% of the microwell array to be filled.<sup>34</sup> Parts e and f of Figure 4 show the portion of a microcapsule array which represents the magnified bright-field and fluorescence images of the entrapped microcapsules, respectively. Microcapsules encapsulating *B. braunii* cells were readily distinguishable from empty microcapsules by fluorescence microscopy. The differences in lipid

content among the three microalgae in the microwells were estimated by their fluorescence (Figure 4g).

**Viability Assessment.** A cell viability assay was performed to see if the algal cell is actually live in the microcapsule. Parts a and b of Figure 5 present bright-field and fluorescence

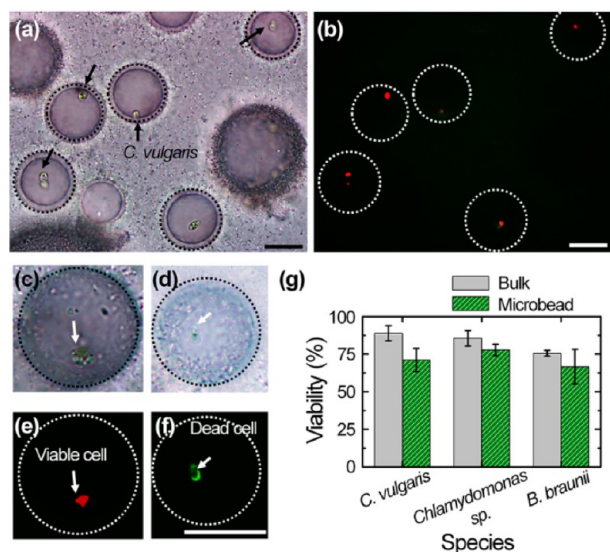


**Figure 5.** Viability of the three microalgae species. (a) Bright-field and (b) fluorescence micrographs of encapsulated *C. vulgaris* cells stained with SYTOX green. Magnified bright-field images of microcapsules containing single (c) live and (d) dead microalgae, which emit (e) red and (f) bright green fluorescence due to SYTOX green staining. Scale bars: 20  $\mu\text{m}$ . (g) Percentage of live cells in bulk samples ( $n = 30$ ) and within microcapsules ( $n = 15$ ) of the three species.

microscopic images, respectively, of encapsulated *C. vulgaris* cells stained with SYTOX green. *C. vulgaris* was readily visualized by its red fluorescence. Images of single-alga-containing microcapsules showed that live (Figure 5, parts c and e) and dead cells (Figure 5, parts d and f) were distinguishable by their red and bright green colors, respectively. Two distinct fluorescence signals after SYTOX staining of the other species (*Chlamydomonas* sp. and *B. braunii*) were also observed (data not shown). We also quantified microalgae viability (Figure 5g) both in bulk and within microcapsules. The viabilities of free *C. vulgaris*, *Chlamydomonas* sp., and *B. braunii* cells were 88.88%, 85.56%, and 75.56%, respectively, based on three replicates. Despite the acidity and low gas permeability of oleic acid, the percentage viabilities of *C. vulgaris*, *Chlamydomonas* sp., and *B. braunii* within the microcapsule were stable at  $\sim 70\%$ . This was because oleic acid was exchanged for mineral oil at the microfluidic collection chamber, resulting in maintenance of cell viability within the alginate microcapsules. The viability of cells within alginate hydrogel microcapsules could be further improved by introduction of pure oil, such as mineral oil or hexadecane, as a control flow through the additional oil exchange microchannel.<sup>30</sup> A microfluidic device that enables continuous-flow extraction of microcapsules from an oil phase into aqueous phase might also increase the viability.

## DISCUSSION

We determined the lipid content of single microalgal cells within alginate hydrogel microcapsules. Many microalgae accumulate lipids under environmental stresses, including

nitrogen repletion, UV exposure, low light, temperature, salt stress, and nutrient deficiency. In particular, nutrient deficiency has a marked effect on algal lipid content.<sup>5,35,36</sup> Thus, several studies of the effects of nutrient deficiency have been reported; however, the results reflected only the average lipid content of algal communities in response to an external stress. The advantage of microcapsule-based determination of the lipid content of a single cell rather than in bulk is that the effect of environmental stress on individual microalgal cells can be determined. The immediate response of a single live alga to a shift in environmental conditions could be monitored in real time by fluorescence microscopy. Furthermore, the integration of microfluidic components for microcapsule storage in the microwell array (Figure 4) and mounting of a microchannel to supply various chemical reactants to the individual microcapsules may provide a multiplexed screening platform for studies of individual algal cells. This approach will facilitate the discovery of cellular heterogeneity in algal cultures, which has been investigated only in bulk systems to date.

The heterogeneity in lipid content shown in Figure 4 is derived from the variability in cell status according to growth rate. Light is important for growth of algae, which ensures high lipid productivity via photosynthesis. However, bulk cultivation in 250 mL conical shaking flasks, rotating at 120 rpm under continuous illumination, suffers from insufficient light provision due to the high cell density. Cells deeper in the shaking flask receive attenuated light, less than the average light intensity per cell.<sup>37</sup> This “self-shading” effect would be greater in larger culture flasks as the cell density increases. This effect results in differences in growth rate and lipid accumulation among cells according to their position in the flask. This in turn leads to the difference in BODIPY fluorescence intensity.

Successful biodiesel production depends on the selection of fast-growing, lipid-rich microalgae from a large number of microalgal species. Thus, the lipid content of an individual alga should be determined. Lipid-rich microalgae are generally identified using fluorescence-activated cell sorting (FACS), which can distinguish lipid-stained from unstained cells in a high-throughput manner. The combination of BODIPY staining with green fluorescence and FACS allows effective cell separation because the emission spectrum of BODIPY is spectrally separated from the red algal autofluorescence. However, use of FACS has some limitations. First, monitoring and measuring the behavior of individual cells is problematic. Also, typical FACS systems are expensive to purchase and maintain, and they require highly trained operators, making it problematic for environmental engineers to operate the complicated apparatus. The most important problem is that FACS does not ensure the viability of recovered cells. Post-FACS cells have a higher probability of damage and contamination, referred to as “cross-contamination”. On the other hand, using droplet-based microfluidics, a single alga can be encapsulated into a picoliter droplet. In particular, the proposed platform provides an appropriate environment for live microalgae within the hydrogel microcapsule with a continuous supply of culture medium, while avoiding cross-contamination from other microorganisms. Many suitable droplet-based microfluidics approaches for continuous droplet sorting based on cellular fluorescence signals have been reported; these facilitate recovery and inoculation of the cells of interest. The stochastic heterogeneity in algal lipid content, which was estimated quantitatively in our system, is a critical selection criterion for a specific microalga with high lipid



content. Furthermore, automated or interactive selection of a microcapsule containing the desired alga with no need for complex apparatus is required in various environmental technologies. An optoelectrofluidic interactive separation technique<sup>38</sup> would be appropriate for this purpose. Currently, we are attempting to develop an optoelectrofluidic manipulation platform for the facile selection of individual hydrogel microcapsules containing single microalgae. On the basis of the optically induced dielectrophoretic force, the microcapsules entrapped in the microwell array can be retrieved selectively using an optoelectrofluidic interactive manipulation technology.

## CONCLUSION

In the current study, we successfully encapsulated microalgal cells within alginate hydrogel-based microcapsules in a microfluidic device that incorporated a microbridge structure. This was confirmed using the microalgae *C. vulgaris*, *Chlamydomonas* sp., and *B. braunii*. To our knowledge, this is the first report that live algae cells could be encapsulated and their lipid contents determined in an online, real-time manner. By utilizing the rapid migration of the additional control flow, which includes a calcified oil phase, via a microbridge structure, we could fabricate stable alginate hydrogel microcapsules with suitable spacing; moreover, no aggregation of microcapsules was identified. The fabricated microcapsules showed characteristics of monodispersity, sufficient robustness in handling, stability for long-term manipulation, and maintenance of cell viability.

This unique combination of microcapsules and non-destructive fluorescence staining with BODIPY will facilitate follow-up biological analyses. Similar to previous reports, the fluorescence intensity differed significantly among the three species due to differences in lipid contents. The heterogeneity of lipid accumulation among individual cells of the same species was investigated by in situ profiling of the intercellular lipid at the single-cell level. We also combined the cell-encapsulation methodology with the microwell array technology to realize a lipid screening platform. Maintenance of cell viability within the microcapsules was confirmed by SYTOX staining. Therefore, microcapsule encapsulation protected the cells from damage during lipid screening procedures. The proposed microcapsule-based platform for screening of lipid-rich microalgae is now ready for use in alternative energy development and represents a versatile tool for environmental engineering research.

## ASSOCIATED CONTENT

### Supporting Information

Individual profiling of single cells in three species (Figure S1) as noted in text. This material is available free of charge via the Internet at <http://pubs.acs.org>.

## AUTHOR INFORMATION

### Corresponding Author

\*E-mail: [jekyun@kaist.ac.kr](mailto:jekyun@kaist.ac.kr). Phone: +82-42-350-4315. Fax: +82-42-350-4310.

### Notes

The authors declare no competing financial interest.

## ACKNOWLEDGMENTS

This research was supported by a National Leading Research Laboratory Program (Grant NRF-2013R1A2A1A05006378), a Nano/Bio Science and Technology Program (Grant NRF-

2005-2001291), an NRF Program (Grant NRF-2012M1A2A2026587), and a Converging Research Center Program (Grant 2011K000864) through the National Research Foundation of Korea funded by the Ministry of Science, ICT and Future Planning.

## REFERENCES

- (1) Hill, J.; Nelson, E.; Tilman, D.; Polasky, S.; Tiffany, D. *Proc. Natl. Acad. Sci. U.S.A.* **2006**, *103*, 11206–11210.
- (2) Chisti, Y. *Biotechnol. Adv.* **2007**, *25*, 294–306.
- (3) Wijffels, R. H.; Barbosa, M. J. *Science* **2010**, *329*, 796–799.
- (4) Lim, J. K.; Chieh, D. C. J.; Jalak, S. A.; Toh, P. Y.; Yasin, N. H. M.; Ng, B. W.; Ahmad, A. L. *Small* **2012**, *8*, 1683–1692.
- (5) Rodolfi, L.; Chini Zittelli, G.; Bassi, N.; Padovani, G.; Biondi, N.; Bonini, G.; Tredici, M. R. *Biotechnol. Bioeng.* **2009**, *102*, 100–112.
- (6) Griffiths, M. J.; Harrison, S. T. L. *J. Appl. Phycol.* **2009**, *21*, 493–507.
- (7) Griffiths, M. J.; van Hille, R. P.; Harrison, S. T. L. *J. Appl. Phycol.* **2012**, *24*, 989–1001.
- (8) Di Carlo, D.; Aghdam, N.; Lee, L. P. *Anal. Chem.* **2006**, *78*, 4925–4930.
- (9) Skelley, A. M.; Kirak, O.; Suh, H.; Jaenisch, R.; Voldman, J. *Nat. Methods* **2009**, *6*, 147–152.
- (10) Kürsten, D.; Cao, J.; Funfak, A.; Müller, P.; Köhler, J. M. *Eng. Life Sci.* **2011**, *11*, 580–587.
- (11) Lefevre, F.; Chalifour, A.; Yu, L.; Chodavarapu, V.; Juneau, P.; Izquierdo, R. *Lab Chip* **2012**, *12*, 787–793.
- (12) Jung, E. E.; Kalontarov, M.; Doud, D.; Ooms, M.; Angenent, L.; Sinton, D.; Erickson, D. *Lab Chip* **2012**, *12*, 3740–3745.
- (13) Chen, M.; Mertiri, T.; Holland, T.; Basu, A. S. *Lab Chip* **2012**, *12*, 3870–3874.
- (14) Holcomb, R. E.; Mason, L. J.; Reardon, K. F.; Crokek, D. M.; Henry, C. S. *Anal. Bioanal. Chem.* **2011**, *400*, 245–253.
- (15) Mu, X.; Zheng, W.; Sun, J.; Zhang, W.; Jiang, X. *Small* **2013**, *9*, 9–21.
- (16) Grier, D. G. *Nature* **2003**, *424*, 810–816.
- (17) Bausch, A. R.; Möller, W.; Sackmann, E. *Biophys. J.* **1999**, *76*, 573–579.
- (18) Charnley, M.; Textor, M.; Khademhosseini, A.; Lutolf, M. P. *Integr. Biol.* **2009**, *1*, 625–634.
- (19) Dewan, A.; Kim, J.; McLean, R. H.; Vanapalli, S. A.; Karim, M. N. *Biotechnol. Bioeng.* **2012**, *109*, 2987–2996.
- (20) Pan, J.; Stephenson, A. L.; Kazamia, E.; Huck, W. T. S.; Dennis, J. S.; Smith, A. G.; Abell, C. *Integr. Biol.* **2011**, *3*, 1043–1051.
- (21) Teh, S. Y.; Lin, R.; Hung, L. H.; Lee, A. P. *Lab Chip* **2008**, *8*, 198–220.
- (22) Ying, D.; Zhang, K.; Li, N.; Ai, X.; Liang, Q.; Wang, Y.; Luo, G. *BioChip J.* **2012**, *6*, 197–205.
- (23) Mazutis, L.; Griffiths, A. D. *Appl. Phys. Lett.* **2009**, *95*, 204103.
- (24) Tumarkin, E.; Kumacheva, E. *Chem. Soc. Rev.* **2009**, *38*, 2161–2168.
- (25) Um, E.; Lee, D. S.; Pyo, H. B.; Park, J. K. *Microfluid. Nanofluid.* **2008**, *5*, 541–549.
- (26) Morimoto, Y.; Tan, W.; Tsuda, Y.; Takeuchi, S. *Lab Chip* **2009**, *9*, 2217–2223.
- (27) Roy, D.; Greenlaw, P. N.; Shane, B. S. *J. Environ. Sci. Health* **1993**, *28*, 37–50.
- (28) Twist, H.; Edwards, A. C.; Codd, G. A. *Water Res.* **1997**, *31*, 2066–2072.
- (29) Govender, T.; Ramanna, L.; Rawat, I.; Bux, F. *Bioresour. Technol.* **2012**, *114*, 507–511.
- (30) Lee, D. H.; Lee, W.; Um, E.; Park, J. K. *Biomicrofluidics* **2011**, *5*, 034117.
- (31) Um, E.; Lee, S. G.; Park, J. K. *Appl. Phys. Lett.* **2010**, *97*, 153703.
- (32) Huang, G.-H.; Chen, G.; Chen, F. *Biomass Bioenergy* **2009**, *33*, 1386–1392.
- (33) Xu, D.; Gao, Z.; Li, F.; Fan, X.; Zhang, X.; Ye, N.; Mou, S.; Liang, C.; Li, D. *Bioresour. Technol.* **2013**, *127*, 386–390.



- (34) Um, E.; Rha, E.; Choi, S. L.; Lee, S. G.; Park, J. K. *Lab Chip* **2012**, *12*, 1594–1597.
- (35) Yeh, K. L.; Chang, J. S. *Biotechnol. J.* **2011**, *6*, 1358–1366.
- (36) Praveenkumar, R.; Shameera, K.; Mahalakshmi, G.; Akbarsha, M. A.; Thajuddin, N. *Biomass Bioenergy* **2012**, *37*, 60–66.
- (37) Shigesada, N.; Okubo, A. *J. Math. Biol.* **1981**, *12*, 311–326.
- (38) Hwang, H.; Choi, Y. J.; Choi, W.; Kim, S. H.; Jang, J.; Park, J. K. *Electrophoresis* **2008**, *29*, 1203–1212.